FLORE
Repository istituzionale dell'Università degli Studi di Firenze

Effect of size disparity on the structure and dynamics of the small component in concentrated binary colloidal mixtures

(Article begins on next page)

08 January 2025

Effect of size disparity on the structure and dynamics of the small component in concentrated binary colloidal mixtures

E. Martinez-Sotelo,[1] M.A. Escobedo-Sánchez,[2] and M. Laurati[1, 3, a)]

[1)]*División de Ciencias e Ingenierás, Universidad de Guanajuato, Loma del Bosque 103, 37150 León, México*

[2)]*Soft Matter Laboratory, Heinrich-Heine University, Universitätsstrasse 1, 42150 Düsseldorf, Germany*

[3)]*Department of Chemistry "Ugo Schiff" and CSGI, University of Florence, Sesto Fiorentino, Florence I-50019, Italy*

(Dated: 31 October 2019)

We determined, using confocal microscopy, the structure and dynamics of the small component in concentrated binary colloidal mixtures with moderate and large size ratios and different compositions of PMMA particles. We show that when increasing the content of small spheres at fixed total volume fraction, a transition in the local environment of the small particles is observed, from a mixed environment of other small and large particles to a local environment of only small particles. The transition is rather abrupt for moderate size ratios, while it becomes particularly broad for large size ratios. This can be associated to the improved ability of the small particles to pack in between the large particles for larger size ratios. The dynamics reflect the transition with an increase of the mobility observed at intermediate mixing. This increase becomes particularly pronounced for large size ratios, leading to diffusive dynamics of the small particles, in agreement with predictions of theories of the glass transition in binary hard-sphere mixtures. The composition at which the fastest dynamics are observed is apparently independent of the size ratio.

I. INTRODUCTION

Dispersions of bidisperse colloidal hard-spheres are the simplest model system of complex multi-component dispersions[1,2]. The equilibrium state diagram of such mixtures has been studied in detail in the past, as a function of the composition and the size ratio of the components[3–8]. Compared to one-component dispersions, binary mixtures present a broader fluid–solid coexistence region, which has been thoroughly investigated in experiments[9–12]. Additionally, formation of complex crystalline structures through co-crystallization of the two species is predicted and observed[13–16]. However, especially at high packings, these systems fall out of equilibrium. Highly packed states of mixtures are interesting for applications since a large quantity of material occupies a relatively small volume. Glasses of concentrated binary mixtures of hard-sphere like colloids have been also studied recently[11,17–24]. It has been shown in particular that mixing colloids of sufficiently different size can substantially affect the formation of glasses. If the constituents present a moderate size ratio, the glass transition shifts to larger total volume fractions at intermediate composition compared to a mono-component system. When the disparity becomes larger, the formation of mixed states occurs, with the largest component forming a glass in which the small component remains mobile[11,17–23,25–28]. In the regime of mixed states, complex and anomalous dynamic phenomena have been observed[29,30], under conditions which are particularly relevant for realistic systems such as cellular[31] or ionic liquids[32], among others. Due to technical difficulties related with the limited optical resolution of confocal microscopy, or the complexity of introducing selectivity in scattering techniques, experimental characterization of the structure and dynamics of concentrated binary colloidal mixtures has mainly focused on the study of the large component[23,25–28], with a few exceptions in which, however, only the dynamics of the small particles for specific size ratios or a limited number of compositions were investigated[11,24,29,30]. Here we report a systematic experimental investigation of the microscopic structural organization and the single-particle dynamics of the small component in glassy binary colloidal mixtures with moderate to large size ratios and different compositions. We find that while at moderate size ratios the small particles change abruptly from being trapped by a mixture of other small and large spheres to being trapped by only small particles, at intermediate and large size ratios the transition is more gradual due to the ability of the small particles to fill the gaps in between the large particles. This results also in an increase of the mobility of the small particles at intermediate composition.

II. MATERIALS AND METHODS

A. Samples

Mixtures of Polymethyl-methacrylate (PMMA) colloids sterically stabilized with polyhydroxy-stearic acid (PHSA), synthetized according to[33], were dispersed in a density and refractive index matching solvent composed of Bromocyclo-heptane (CHB7) and cis-Decahydronaphthalene (cis-Decalin) (Sigma-Aldrich). Previous to use, Bromocycloheptane was filtered through Aluminum Oxide (Sigma-Aldrich) in order to minimize the amount of charges in the solvent[34]. A 4mM concentration of Tetrabutylammonium chloride (TBAC) salt, corresponding to oversaturated conditions, was added to the

[a)]Electronic mail: mlaurati@fisica.ugto.mx

solvent in order to screen charges on the PMMA particles. Under these conditions, particles still retain a certain amount of charge[35]. In recent work[36] using the same solvent mixture and comparable amounts of added salt, we could estimate the parameters of the electrostatic interaction through comparison with simulations in which a Yukawa potential was used to describe the electrostatic repulsion. We obtained $\kappa R \approx 30$ for an effective particle charge $Z = 500e$. For the small particles, this indicates an inverse screening length $\kappa^{-1} \approx 50$ nm. Previous work also under similar conditions[37] showed that the fluid-crystal coexistence region is found for $0.45 < \phi < 0.54$, indicating that the residual charges induce moderate deviations from hard-sphere behavior. Small particles with an average radius $R_s = (0.80 \pm 0.01)\,\mu m$ (polydispersity 0.07) were mixed with 3 different batches of large particles with average radii $R_{L1} = (1.50 \pm 0.03)\,\mu m$ (polydispersity 0.06), $R_{L2} = (2.25 \pm 0.05)\,\mu m$ (polydispersity 0.06) and $R_{L3} = (3.0 \pm 0.05)\,\mu m$ (polydispersity 0.05). The average radii and polydispersities were obtained by Dynamic Light Scattering (DLS).[38] Accordingly, mixtures with size ratios $\delta = R_s/R_{Li} = 0.53, 0.35$ and 0.26, with $i = 1, 2, 3$ were obtained. Only the small particles were fluorescently labeled with monomerized Rhodamine-B. Rhodamine PMMA monomers were chemically attached to the particles in order to enhance the Dye distribution over the particle. Due to the large size of the particles used to prepare the mixtures, particular care was taken to verify the density matching condition. For all particles, the solvent composition was adjusted until the dispersions did not show any sign of sedimentation over a period of 8 hours when centrifuged at an equivalent gravity of approximately $1341\times g$ at $T = 23$ C, corresponding to the temperature at which the experiments were later performed. Dispersions with total volume fraction $\phi = 0.60$ were prepared by diluting a sediment obtained by centrifuging the particles at $T = 35$ C. The higher temperature was used to alter the density matching condition and allow the particles to sediment. The volume fraction of the random-close packed sediment was assumed to be $\phi_{RCP} = 0.65$ in all cases, according to studies on the effect of polydispersity on random close packing[39]. Samples with different compositions $x_s = \phi_s/\phi$, where ϕ_s is the relative volume fraction of small particles, were obtained by mixing proper amounts of dispersions of small and large particles. After preparation, samples were further mixed in an orbital shaker for one day. Samples were then transferred to a microscopy cell consisting of a small bottle cut at the bottom and glued to a microscope coverslip. Prior to each measurement samples were again gently mixed in order to remove any possible ordering and aging. Possible sample aging occurring during the measurement was neglected.

B. Confocal Microscopy

For each sample, series of image stacks of 100 images of 512x512 pixels, corresponding to a volume of 64x64x20 μm^3 were acquired using a VT-Eye (Visitech) confocal unit mounted on a Nikon Ti-S inverted microscope. A $100\times$ Nikon Plan-Apo VC oil-immersion objective (NA = 1.40) and a laser with $\lambda = 488$ nm were used for image acquisition. Stacks were acquired at a depth of about $20\mu m$ from the coverslip. The time needed to acquire a stack is approximately 3.4 s. For structural investigation, different numbers of volumes in the range from 500 to 2000 (depending on sample) were acquired to obtain satisfactory statistics. For determining the dynamics, time series of 500 stacks were measured for 5 different volumes. Particle coordinates and trajectories were obtained by analyzing the data with standard particle-tracking routines[40].

III. RESULTS AND DISCUSSION

A. Structure of Small Particles

The structure of samples with total volume fraction $\phi = 0.60$ and different size ratios δ and compositions x_s was analyzed through the radial distribution function $g(r)$, which is defined as:

$$g(r) = \frac{N(r)}{4\pi r^2 \Delta r_{sh} n} \ , \tag{1}$$

where $N(r)$ is the number of particles in a thin shell of thickness Δr_{sh} at distance r from a selected particle and n is the total particle number density.

1. Size ratio $\delta = 0.53$

Representative renderings of the small particle positions in sample volumes with $\phi = 0.60$ and different compositions $x_s = 0.01, 0.10, 0.30, 0.50, 0.70$ and 1.00 are shown in Fig.1.

The voids in the volume are occupied by large spheres, as the total volume fraction is large, $\phi = 0.60$. Besides the progressive crowding of the small spheres with increasing x_s, in the samples with the smallest $x_s = 0.01$ and 0.10 one can notice that the small particles are distributed around the whole volume, however they have the tendency of being in contact.

This tendency can be also seen for $x_s = 0.30$, where particles appear to cluster around the voids (the large particles). For $x_s \geq 0.50$ the small particles form increasingly larger and crowded agglomerations, progressively approaching the uniform, crowded distribution of the one-component sample of small spheres, $x_s = 1.00$.

The qualitative analyses based on the volume reconstructions are quantitatively confirmed through the radial distribution functions $g(r)$ (Fig.2). For $x_s = 0.01$ one observes a pronounced first peak corresponding to small particle-small particle contacts (the peak position is approximately at $r/2R_s = 1$. However, the second peak does not correspond to a second shell of small particles: it corresponds instead to a configuration in which two small particles are separated by a large particles, a configuration that is likely to be present for a sample where most of the volume is occupied by large particles.
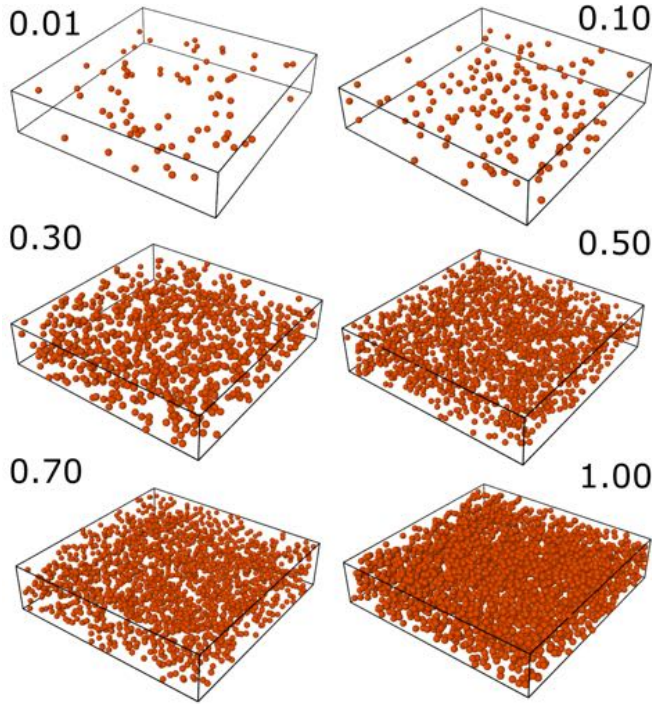
FIG. 1. Renderings of the small particle location in representative volumes of samples with $\delta = 0.53$ and different composition x_s, as indicated.

FIG. 2. Radial distribution functions $g(r)$ as a function of particle-particle distance r, normalized by the particle diameter $2R_s$, for samples with $\delta = 0.53$ and different compositions x_s, as indicated. Curves corresponding to $x_s \geq 0.10$ values are vertically shifted for clarity, each by a factor 1 respect to the previous x_s value. Schematic representations of particle configurations associated with the peaks of $g(r)$ are shown on the top of the graph.

Two additional peaks can be clearly discerned, corresponding to configurations in which two small particles are separated by a large and a small particle or by two large particles. Therefore the structure of the small particles in this sample corresponds to dimers or single particles occupying the voids left by the large particles. For $x_s = 0.10$ a similar pronounced first peak is found, as well as the peaks for which small particles are separated by large particles. However, additionally a small second peak corresponding to a second shell of small particles appears. For $x_s = 0.30$ a significant change is observed: while the peaks corresponding to small particles with large particles in between are still observed, the first peak becomes smaller and broadens to almost reach the distance corresponding to the second shell of small particles. This is indicative of a transition from a structure in which small particles are trapped by a mixture of small and large particles, to a structure in which small particles become surrounded by shells of only other small particles. This transition is evidenced by the sample with $x_s = 0.50$, where now the first and the second peak correspond to the first and second shell of small particles, while the third peak lies in between configurations corresponding to a third shell of small particles and two small particles separated by a large and a small particle. For $x_s = 0.70$ the transition is essentially complete, as confirmed by the close similarity to the $g(r)$ of the sample of only small particles ($x_s = 1.00$). This means that for $x_s = 0.70$ the large particles only act as defects in the small particle structure.
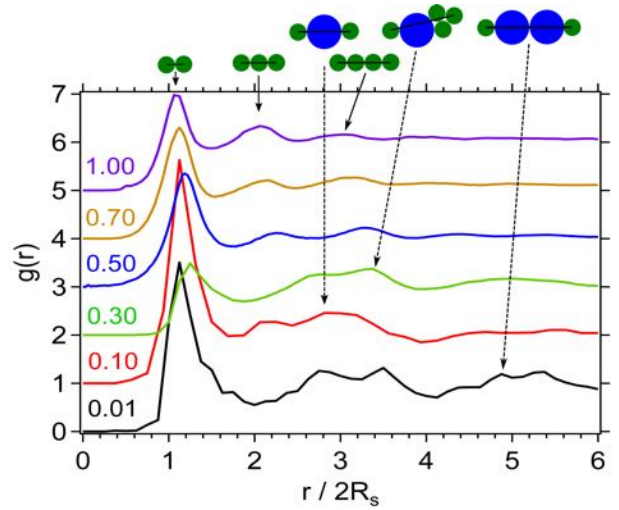
2. Size ratio $\delta = 0.35$

The radial distribution functions of samples with $\phi = 0.60$ and size ratio $\delta = 0.35$ present the same set of particle configurations described for $\delta = 0.53$ (Fig.3). However, the relative contribution of the configurations shows significant differences. For instance, for $x_s = 0.01$ configurations in which small particles are separated by a large particle have the largest probability, more than small particle-small particle contacts. This is shown by the larger height of the second and third peaks of the $g(r)$ compared to the first. Additionally, configurations in which two small particles are separated by two large particles are also likely. The more pronounced mixing between large and small particles can be attributed to the improved ability of smaller particles to fill the voids between large particles. Samples with $x_s = 0.10$ and 0.30 show a progressive growth of the first peak and a related decrease of the second peak. Note that due to the increase in the content of small particles, for $x_s = 0.30$ the second peak corresponds to configurations in which two small particles are separated by a large and a small particle. For $x_s = 0.50$ the first peak is relatively large and the second shell of small particles start to form, however the structure is still considerably different from the system of only small particles, $x_s = 1.00$. This indicates that due to the improved mixing, the transition from a structure in which small and large particles are mixed to a structure in which the large particles act as defects in a dispersion of small particles is smoother than for $\delta = 0.53$. This is confirmed also by sample $x_s = 0.70$, in which the structural organization is not yet completely similar to $x_s = 1.00$.

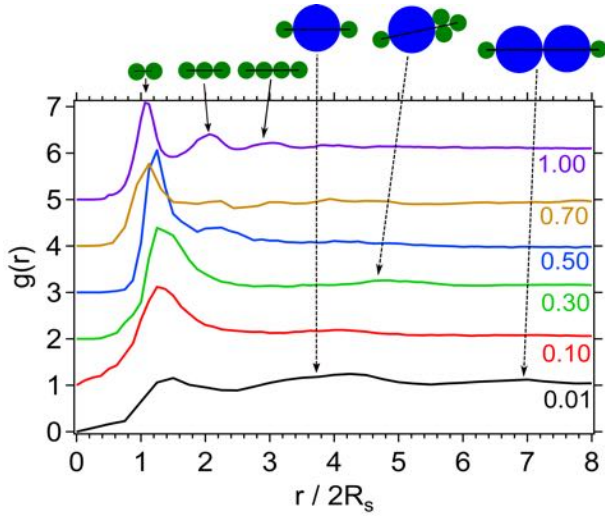The transition from the mixed structure to the formation

FIG. 3. Radial distribution functions $g(r)$ as a function of particle-particle distance r, normalized by the particle diameter $2R_s$, for samples with $\delta = 0.35$ and different compositions x_s, as indicated. Curves corresponding to $x_s \geq 0.10$ values are vertically shifted for clarity, each by a factor 1 respect to the previous x_s value. Schematic representations of particle configurations associated with the peaks of $g(r)$ are shown on the top of the graph.
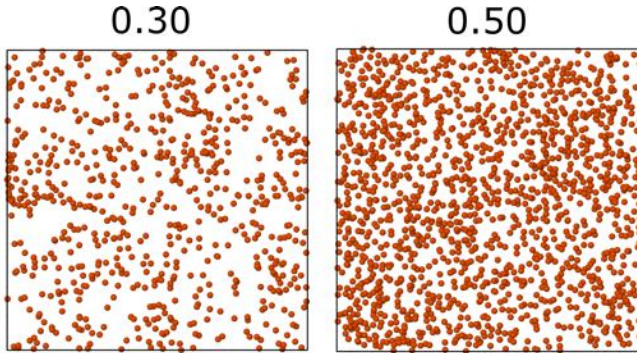
FIG. 4. Renderings of small particles in x-y slices of representative volumes of samples with $\delta = 0.35$ and $x_s = 0.30$ and 0.50.

FIG. 5. Top: Radial distribution functions $g(r)$ as a function of particle-particle distance r, normalized by the particle diameter $2R_s$, for samples with $\delta = 0.26$ and different compositions x_s, as indicated. Curves corresponding to $x_s \geq 0.10$ values are vertically shifted for clarity, each by a factor 1 respect to the previous x_s value. Schematic representations of particle configurations associated with the peaks of $g(r)$ are shown on the top of the graph. Bottom: Representative x-y image slice of sample $x_s = 0.50$. Only the small particles are labeled and visible in the image.

of a second shell of small particles is directly visible in the renderings of representative x-y slices of volumes of samples $x_s = 0.30$ and 0.50 (Fig.4). As can be seen in the sample with $x_s = 0.30$ mostly dimer-like structures are observed, separated by empty regions occupied by large particles, while for $x_s = 0.50$ larger chains and some more isotropic arrangements of particles are present.

3. Size ratio $\delta = 0.26$

The structural arrangement of the small particles for with $\phi = 0.60$ and size ratio $\delta = 0.26$, represented by the pair distribution functions in Fig.5, indicates an even smoother transition to a glass dominated by the small particles. For $x_s = 0.01$
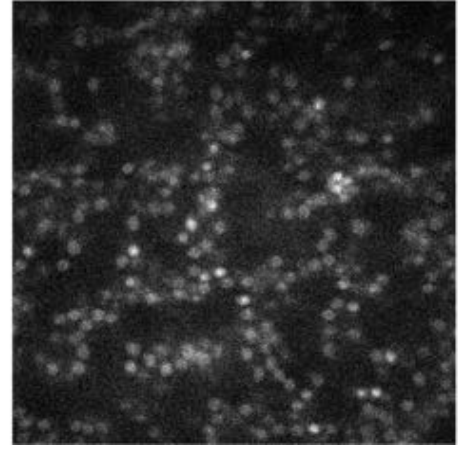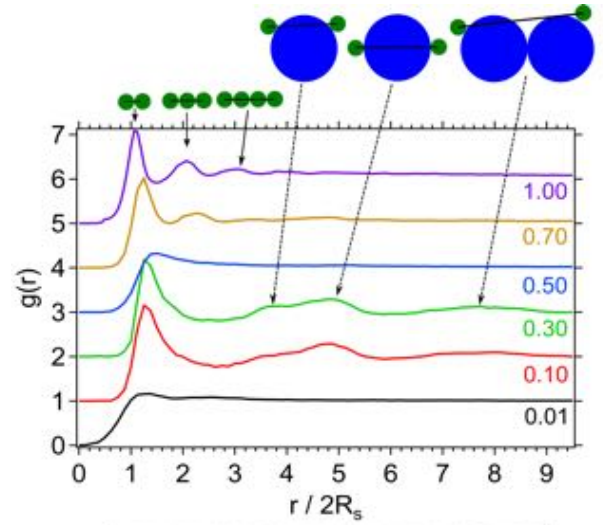
the most probable configurations correspond to two small particles in contact or separated by a large particle. The region of the second peak is particularly broad indicating a large distribution of distances. For $x_s = 0.10$ and 0.30 small particle-small particle contacts are likely, together with configurations where two small particles are separated by a large particle. Interestingly the second peak is characteristic of configurations corresponding to distances between small particles separated by large particles, however not along the diameter of the large particle (see sketch on top of Fig.5). This suggests ring-like structures of the small particles surrounding a large particle. The $g(r)$ of $x_s = 0.50$ is particularly interesting: It shows an extremely broad and unique peak which indicates that all particle configurations have very similar probability. This is in-

dicative of a very mild transition to the structure dominated by a local neighborhood of small particles. The competition between the transition to a local neighborhood of small particles and the occupation of the free space between large particles in sample $x_s = 0.50$ is highlighted by the representative x-y slice image reported in Fig.5. The mild transition is confirmed by the sample with $x_s = 0.70$ where the first two peaks correspond to the first two shells of small particle neighbors, while the third and fourth peak still correspond to configurations where small particles are separated by large particles. Therefore the larger size ratio associated with the improved ability of the small particles to fill gaps between large particles, leads to a very broad transition in caging mechanism.

B. Dynamics of Small Particles

The dynamics of the small particles in mixtures with total volume fraction $\phi = 0.60$ and different size ratio δ and composition x_s were investigated at the single particle level by determining the average mean square displacement $\langle \Delta r^2(\Delta t) \rangle$, which is defined as:

$$\langle \Delta r^2(\Delta t) \rangle = \langle (r_i(\Delta t + t_0) - r_i(t_0))^2 \rangle_{t_0,i} , \qquad (2)$$

where Δt is the delay time, t_0 a time during the particle trajectory, $\langle ... \rangle_{t_0,i}$ indicates an average over all times t_0 and all particles i.

1. Size disparity $\delta = 0.53$

The average mean squared displacements (MSD) determined for samples with $\phi = 0.60$ and size ratio $\delta = 0.53$ present in all cases a sub-diffusive behavior, indicative of glassy dynamics (Fig.6). Moreover, for all mixtures the MSD is larger than for the glass of only small particles ($x_s = 1.00$). A non-monotonic behavior of the displacements is observed as a function of x_s: The MSD decreases from $x_s = 0.01$ to 0.10, it then increases for $x_s = 0.30$ and 0.50, where it is maximum and almost diffusive, finally it decreases again for $x_s = 0.70$. This trend is clearly visualized in the inset of Fig.6, where we report $\Delta r^2(t = 50)$ s as a function of x_s. Note that the maximum MSD is observed in correspondence of the transition from a structure in which the neighborhood of a small particle is formed by a mixture of small and large particles to a structure in which the local neighborhood of a small particle is composed of other small particles, as shown by the $g(r)$ of Fig.2.

2. Size ratio $\delta = 0.35$

The MSDs of the small particles obtained for mixtures with $\phi = 0.60$ and $\delta = 0.35$ (Fig.7) and different compositions x_s present generally larger values than corresponding samples with $\delta = 0.53$. This indicates that particles (which have the
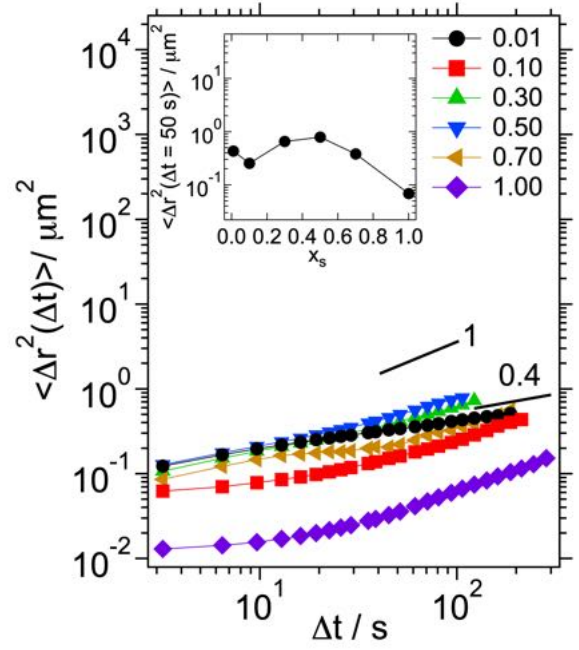

FIG. 6. Mean square displacement of the small particles $\langle Delta r^2(\Delta t) \rangle$ as a function of delay time Δt, for samples with $\delta = 0.53$ and different compositions x_s, as indicated. Inset: $\langle \Delta r^2(\Delta t = 50\,\mathrm{s}) \rangle$ as a function of x_s

FIG. 7. Mean square displacement of the small particles $\langle \Delta r^2(\Delta t) \rangle$ as a function of delay time Δt, for samples with $\delta = 0.35$ and different compositions x_s, as indicated. Inset: $\langle \Delta r^2(\Delta t = 50\,\mathrm{s}) \rangle$ as a function of x_s

same size as for $\delta = 0.53$) can explore larger volumes. The dependence on x_s is similar to the previous size ratio, with maximal displacements observed for $x_s = 0.50$. However, the variation of mobility for this size ratio is larger (inset of Fig.7) and the dynamics for $x_s = 0.30$ and 0.50 are in this case diffusive at long times, This indicates a fluid-like state for the small particles at intermediate composition. As for the previous size ratio, the maximal displacements are observed in correspondence to the transition in the local neighborhood of a small particle.

3. Size ratio $\delta = 0.26$

For the mixtures with $\phi = 0.60$ and the largest size ratio $\delta = 0.26$ we observe even larger displacements compared to
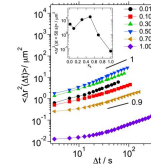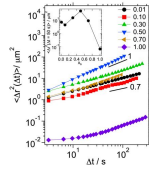
FIG. 8. Mean square displacement of the small particles $\langle \Delta r^2(\Delta t) \rangle$ as a function of delay time Δt, for samples with $\delta = 0.26$ and different compositions x_s, as indicated. Inset: $\langle \Delta r^2(\Delta t = 50\,\text{s}) \rangle$ as a function of x_s

the previous cases (Fig.8). The dependence of the MSD on x_s at fixed time is similar to the other disparities. However, the variation is the largest. Similar to $\delta = 0.35$, the dynamics for $x_s = 0.50$ are the fastest and diffusive, indicating a fluid state of the small particles.

IV. DISCUSSION

The experimentally determined information on the structural organization of the small particles in glassy binary mixtures complements the experimental findings reported in previous work on the structural organization of the large particles for similar volume fractions $\phi = 0.58$ and 0.61, and $\delta = 0.20^{23,26,41,42}$. In particular, these previous studies evidenced a caging transition for the large particles from a cage formed by other large particles to a cage formed by small particles, occurring around $x_s = 0.50$. The results presented here for $\delta = 0.26$ indicate that this transition coincides with the formation of a local neighborhood of small particles around each small particle, i.e. the onset of the formation of a cage of small particles surrounding a small particle. Compared with results of simulations for the $g(r)$ of the small particles for $\phi = 0.58$ and $\delta = 0.2^{42}$, our results for $\delta = 0.26$ indicate for small values of x_s a more mixed structure of small and large spheres: In^{42} indeed the cage of small spheres starts to form already at $x_s = 0.30$, while here for $x_s > 0.50$. This difference might be due to the smaller size ratio ($\delta = 0.2$) and volume fraction ($\phi = 0.58$) investigated in^{42}, which might favor the formation of locally crowded regions of small particles in the voids left by the large particles. It might also be affected by the absence of polydispersity in the simulation data. In Ref.^{30} simulation results on the structure factor $S(q)$ of the small particles for $\phi = 0.62$ and $\delta = 0.20$ showed that small particle-small particle correlations and the average distance between small particles increased going from $x_s > 0.01$ to $x_s > 0.10$. Similar results were also observed in simulations of glassy mixtures of soft spheres^{17}. Here we observe a similar trend going from $x_s > 0.01$ to 0.50 for $\phi = 0.60$ and $\delta = 0.26$ (Fig.5). We interpret this trend as associated with the transition to a neighborhood of small spheres, leading to a progressively broad distribution of inter-particles distances, before cages of small spheres around small (and large) spheres are formed. Our study of different size ratios δ in addition shows that

larger size ratio leads to a broader and smoother transition in the local neighborhood of the small spheres, which we associate with the improved ability of the small spheres to fill the empty spaces left by the large spheres.

The increase in the MSD with increasing size ratio demonstrated by Figs.6,7,8 is in agreement with simulation results on hard sphere mixtures reported in^{29,30} for $\delta = 0.20$ and 0.35 and comparable ϕ, and with simulations of soft spheres for intermediate x_s and $0.1 < \delta < 0.9^{18}$. The decrease in the displacements for increasing x_s from 0.01 to 0.10 and the sub-diffusive dynamics for $x_s = 0.01$ are in agreement with results in^{30}. Moreover, the increased small particle dynamics at intermediate composition are in agreement with simulations of glassy dispersions of soft spheres^{17}. A recent work of Voigtmann and Horbach^{32} highlighted the role of small particle-small particle interactions, increasing with increasing x_s, in the speed-up of the dynamics. Previous reports have shown that the dynamics of the large particles for $\phi = 0.58$ and 0.61, and $\delta = 0.20$ present a maximum at $x_s = 0.30^{26,41,42}$ and are also pronounced for $x_s = 0.50$. Our closest data obtained for $\delta = 0.26$ indicate that the dynamics of the small spheres show a maximum for $x_s = 0.50$ and are also pronounced for $x_s = 0.30$ (in agreement with results in Ref.^{24}). This suggests, as also discussed in Ref.^{17,24,30}, a coupling between the dynamics of the small and large particles. It is interesting to note the shift in the composition of the largest mobility between large and small spheres, which however might be affected by the different size ratio. Finally, our data show that the maximum mobility of the small particles is observed in all cases for $x_s = 0.50$, independent of the size ratio. This is different from the behavior of the linear viscoelastic storage modulus, which shows a δ dependent minimum^{42}. It suggests, as also discussed in Ref.^{42}, that the rheological properties are determined by the interplay of the dynamics of the small and large particles.

We compare our results with predictions of the Self-Consistent Generalized Langevin Equation (SCGLE) theory^{21,24} (Fig.9) and Mode Coupling Theory (MCT)^{22,42} (Fig.10). In the case of SCGLE, for $\delta = 0.53$ we compare our results with the state diagrams available from the literature^{21} for $\delta = 0.4$ and 0.6 (Fig.9a). We should note that the state diagrams in^{21} are reported in terms of the volume fraction normalized by the volume fraction at which the glass transition is observed in the one component system (ϕ_g) against the molar fraction of the small spheres (ξ_s). For comparison we thus assumed $\phi_g = 0.58^{38}$ and calculated $\xi_s = x_s[\delta^3 + x_s(1 - \delta^3)]^{-1}$.^{25} The samples with intermediate compositions are the ones closest to the global glass transition line for $\delta = 0.6$ and deeper in the fluid state for $\delta = 0.4$. A similar result is observed for the comparison with the MCT state diagram for $\delta = 0.5$ taken from Ref.^{22}: The intermediate compositions are the closest to the glass melting line. For $\delta = 0.35$ we compare with the SCGLE state diagrams with $\delta = 0.3$ and 0.4^{21} (Fig.9b). In this case all intermediate compositions $0.1 \leq x_s \leq 0.9$ are expected to lie within the fluid state. However, assuming a glass transition line comprised between the limiting cases of $\delta = 0.3$ and
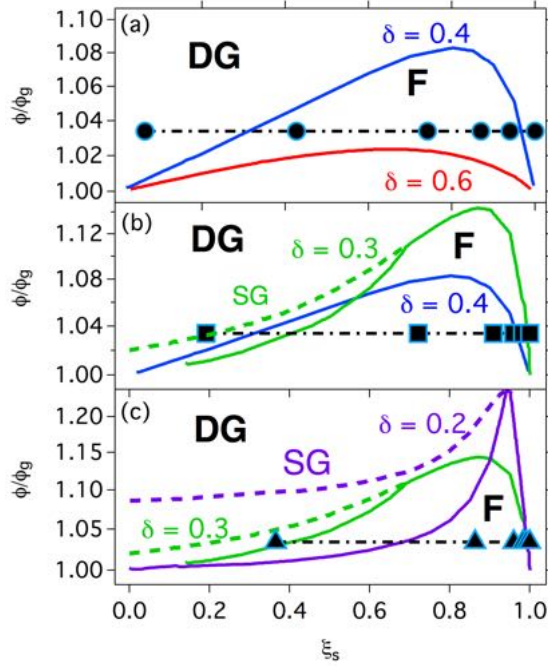
FIG. 9. Comparison between experimental data (symbols) and SC-GLE state diagrams for samples with (a) $\delta = 0.53$, (b) $\delta = 0.35$ and (c) $\delta = 0.26$. The δ values of the SCGLE state boundaries are indicated in the plots. Solid lines indicate boundaries between fluid (F) and double glass (DG) or single glass (SG) states. Dashed lines indicate boundaries between double and single glasses. The x-axis reports th molar fraction ξ_s.
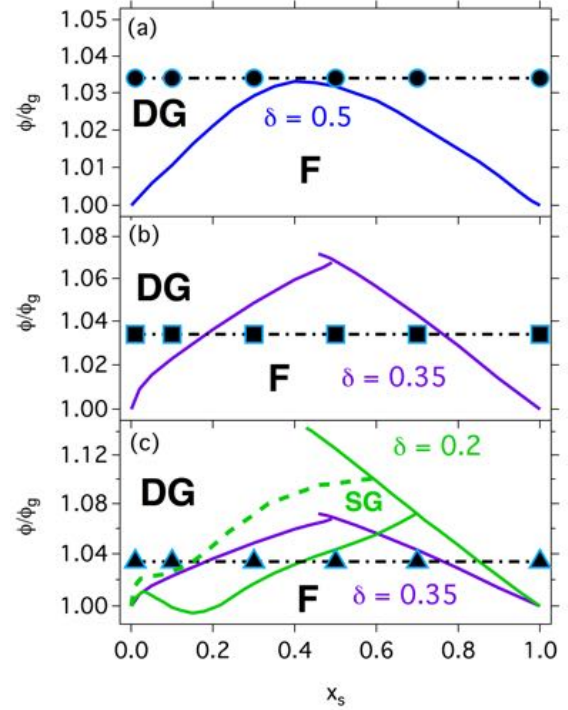

FIG. 10. Comparison between experimental data (symbols) and MCT state diagrams for samples with (a) $\delta = 0.53$, (b) $\delta = 0.35$ and (c) $\delta = 0.26$. The δ values of the MCT state boundaries are indicated in the plots. Solid lines indicate boundaries between fluid (F) and double glass (DG) or single glass (SG) states. Dashed lines indicate boundaries between double and single glasses.

0.4, one might expect the composition with $x_s = 0.3$ to be deeper in the fluid states, i.e. farther from the glass melting line inside the fluid region. On the other hand the comparison with the MCT state diagram for $\delta = 0.35$[22] shows again that for $x_s = 0.5$ the system is expected to be deeper in the fluid state. Finally, for $\delta = 0.26$ we compare with the SCGLE state diagrams with $\delta = 0.2$ and 0.3[21] (Fig.9c), and with the MCT state diagrams with $\delta = 0.2$ and 0.35[22] (Fig.10c). The comparison with SCGLE indicates similar to the case $\delta = 0.35$ that the intermediate composition should lie within the single glass state (where the small particles are mobile) of the fluid state. However assuming again that the state diagram for $\delta = 0.26$ should lie in between the ones for $\delta = 0.2$ and 0.3, one might expect that samples with $x_s = 0.1$ or 0.3 are deeper in the fluid state than $x_s = 0.5$. In the case of MCT, assuming in this case a behavior intermediate between the state diagrams for $\delta = 0.2$ and 0.35, but closer to 0.2, the sample with $x_s = 0.5$ would be the one which has the larger distance from the double glass, or global, transition line. In summary, comparison with theories, in particular with MCT, indicate that the largest mobility of the small particles can be linked to the largest distance from the double glass for fluid states ($\delta = 0.26$ and 0.35) or to the closest vicinity to it when in the glass state ($\delta = 0.53$). It thus suggests, as commented before in the comparison with simulations, that the coupling between the dynamics of the small and large particles plays

an important role.

V. CONCLUSIONS

We experimentally determined the structure and dynamics of small particles in glassy binary mixtures of hard-sphere colloids as a function of the composition of the mixture and for different size ratio. For all size ratios we observe a transition in the local neighborhood of the small particles from configurations in which a small particle is surrounded by both large and small particles, to configurations in which the first shell of neighbors, i.e. the cage, are only composed of small particles. The transition starts for a composition $x_s = 0.30$ in all cases. However, the extension of the transition in the local structure of the small particles changes significantly for different size ratios. It is rather narrow for $\delta = 0.53$, the smallest size ratio, where a local neighborhood of other small particles is already formed at $x_s = 0.50$. It becomes increasingly broader for the larger disparities $\delta = 0.35$ and 0.26, where even at $x_s = 0.70$ the transition is incomplete. This is possibly associated with the improved ability of the small particles to occupy the voids in between large particles for larger size ratio. The structural transition is reflected in the dynamics of the small particles, which for all samples present a non-monotonic dependence

on composition x_s, with a maximum at intermediate mixing, around $x_s = 0.50$. Interestingly, the composition of the fastest dynamics does not seem to depend on size ratio. However, for larger size ratios the increase of mobility at intermediate mixing becomes increasingly pronounced, leading to diffusive dynamics for $x_s = 0.50$. Comparison with theoretical predictions of MCT and SCGLE[21,22,24] indicates that the maximum mobility of the small spheres corresponds to the maximal distance from the double glass transition line, suggesting an important coupling between the dynamics of the small and large particles.

ACKNOWLEDGMENTS

[1] W. Russel, D. Saville, and W. Schowalter, *Colloidal Dispersions*, Cambridge Monographs on Mechanics (Cambridge University Press, 1989).

[2] J. Mewis and N. J. Wagner, *Colloidal Suspension Rheology* (Cambridge University Press, Cambridge, 2012).

[3] M. Dijkstra, R. van Roij, and R. Evans, Phys. Rev. E **59**, 5744 (1999).

[4] B. Götzelmann, R. Roth, S. Dietrich, M. Dijkstra, and R. Evans, Europhys. Lett. **47**, 398 (1999).

[5] R. Roth, R. Evans, and S. Dietrich, Phys. Rev. E **62**, 5360 (2000).

[6] S. Amokrane, A. Ayadim, and J. Malherbe, J. Chem. Phys. **123**, 174508 (2005).

[7] J. G. Malherbe and W. Krauth, Mol. Phys. **105**, 2393 (2007).

[8] D. J. Ashton, N. B. Wilding, R. Roth, and R. Evans, Phys. Rev. E **84**, 061136 (2011).

[9] J. S. van Duijneveldt, A. W. Heinen, and H. N. W. Lekkerkerker, Europhys. Lett. **21**, 369 (1993).

[10] A. D. Dinsmore, A. G. Yodh, and D. J. Pine, Phys. Rev. E **52**, 4045 (1995).

[11] A. Imhof and J. K. G. Dhont, "Experimental phase diagram of a binary colloidal hard-sphere mixture with a large size ratio," Phys. Rev. Lett. **75**, 1662–1665 (1995).

[12] W. J. Hunt and C. F. Zukoski, Langmuir **12**, 6257 (1996).

[13] R. H. O. P. Bartlett and P. N. Pusey, Phys. Rev. Lett. **68**, 3801 (1992).

[14] X. Cottin and P. A. Monson, J. Chem. Phys. **102**, 3354 (1995).

[15] A. B. Schofield, Phys. Rev. E **64**, 051403 (2001).

[16] A.-P. Hynninen, L. Filion, and M. Dijkstra, J. Chem. Phys. **131**, 064902 (2009).

[17] A. J. Moreno and J. Colmenero, "Anomalous dynamic arrest in a mixture of large and small particles," Phys. Rev. E **74**, 021409 (2006).

[18] A. J. Moreno and J. Colmenero, "Relaxation scenarios in a mixture of large and small spheres: Dependence on the size disparity," J. Chem. Phys. **125**, 164507 (2006).

[19] E. Zaccarelli, C. Mayer, A. Asteriadi, C. N. Likos, F. Sciortino, J. Roovers, H. Iatrou, N. Hadjichristidis, P. Tartaglia, H. Löwen, and D. Vlassopoulos, "Tailoring the flow of soft glasses by soft additives," Phys. Rev. Lett. **95**, 268301 (2005).

[20] C. Mayer, E. Zaccarelli, E. Stiakakis, C. N. Likos, F. Sciortino, A. Munam, M. Gauthier, N. Hadjichristidis, H. Iatrou, P. Tartaglia, H. Löwen, and D. Vlassopoulos, "Asymmetric caging in soft colloidal mixtures," Nat. Mat. **7**, 780–784 (2008).

[21] R. Juárez-Madlonado and M. Medina-Noyola, "Theory of dynamic arrest in colloidal mixtures," Phys. Rev. E **77**, 051503 (2008).

[22] Th. Voigtmann, "Multiple glasses in asymmetric binary hard spheres," Europhys. Lett. **96**, 36006 (2011).

[23] J. Hendricks, R. Capellmann, A. B. Schofield, S. U. Egelhaaf, and M. Laurati, "Different mechanisms for dynamical arrest in largely asymmetric binary mixtures," Phys. Rev. E **91**, 032308 (2015).

[24] E. Lázaro-Lázaro, J. A. Perera-Burgos, P. Laermann, T. Sentjabrskaja, G. Pérez-Ángel, M. Laurati, S. U. Egelhaaf, M. Medina-Noyola, T. Voigtmann, R. Castañeda Priego, and L. F. Elizondo-Aguilera, "Glassy dynamics in asymmetric binary mixtures of hard spheres," Phys. Rev. E **99**, 042603 (2019).

[25] T. Sentjabrskaja, E. Babaliari, J. Hendricks, M. Laurati, G. Petekidis, and S. U. Egelhaaf, "Yielding of binary colloidal glasses," Soft Matter **9**, 4524–4533 (2013).

[26] T. Sentjabrskaja, M. Hermes, W. C. K. Poon, C. D. Estrada, R. Castañeda-Priego, S. U. .Egelhaaf, and M. Laurati, "Transient dynamics during stress overshoots in binary colloidal glasses," Soft Matter **10**, 6546–6555 (2014).

[27] T. Sentjabrskaja, M. Laurati, and S. U. Egelhaaf, "One- and two-component colloidal glasses under transient shear," Europ. Phys. J Spec. Topics **226**, 3023–3037 (2017).

[28] T. Sentjabrskaja, J. Hendricks, A. R. Jacob, G. Petekidis, S. U. Egelhaaf, and M. Laurati, "Binary colloidal glasses under transient stress- and strain-controlled shear," J. Rheol. **62**, 149–159 (2018), https://doi.org/10.1122/1.5009193.

[29] T. Sentjabrskaja, E. Zaccarelli, C. De Michele, F. Sciortino, P. Tartaglia, Th. Voigtmann, S. U. Egelhaaf, and M. Laurati, "Anomalous dynamics of intruders in a crowded environment of mobile obstacles," Nature Commun. **7**, 11133 (2016).

[30] M. Laurati, T. Sentjabrskaja, J. Ruiz-Franco, S. U. Egelhaaf, and E. Zaccarelli, "Different scenarios of dynamic coupling in glassy colloidal mixtures," Phys. Chem. Chem. Phys. **20**, 18630–18638 (2018).

[31] F. Höfling and T. Franosch, "Anomalous transport in the crowded world of biological cells," Reports on Progress in Physics **76**, 046602 (2013).

[32] Th. Voigtmann and J. Horbach, "Double transition scenario for anomalous diffusion in glass-forming mixtures," Phys. Rev. Lett. **103**, 205901 (2009).

[33] L. Antl, J. Goodwin, R. Hill, R. Ottewill, S. Owens, S. Papworth, and J. Waters, "The preparation of poly(methyl methacrylate) latices in nonaqueous media," Colloids and Surfaces **17**, 67 – 78 (1986).

[34] M. Leunissen, *Manipulating colloids with charges and electric fields*, Ph.D. thesis, Utrecht University, Utrecht (2007).

[35] C. P. Royall, W. C. P. Poon, and E. R. Weeks, "In search of colloidal hard spheres," Soft Matter **9**, 17–27 (2013).

[36] R. F. Capellmann, N. E. V. Pérez, B. Simon, S. U. Egelhaaf, M. Laurati, and R. Castañeda-Priego, "Structure of colloidal gels at intermediate concentrations: the role of competing interactions," Soft Matter **12**, 9303–9313 (2016).

[37] M. Jenkins, *Quantitative Confocal Microscopy of Dense Colloidal Systems*, Ph.D. thesis, University of Edinburgh, Edinburgh (2005).

[38] P. N. Pusey and W. van Megen, "Detection of small polydispersities by photon correlation spectroscopy," J. Chem. Phys. **80**, 3513–3520 (1984), https://doi.org/10.1063/1.447195.

[39] W. Schaertl and H. Silescu, "Brownian dynamics of polydisperse colloidal hard-spheres - equilibrium structures and random close packings," J. Stat. Phys. **77**, 1007–1025 (1994).

[40] J. C. Crocker and D. G. Grier, "Methods of digital video microscopy for colloidal studies," J. Coll. Interf. Sci. **179**, 298–310 (1996).

[41] T. Sentjabrskaja, D. Guu, M. P. Lettinga, S. U. Egelhaaf, and M. Laurati, "Glasses of dynamically asymmetric binary colloidal mixtures: Quiescent properties and dynamics under shear," AIP Conf. Proc. **1518**, 206 (2013).

[42] T. Sentjabrskaja, A. R. Jacob, S. U. Egelhaaf, G. Petekidis, T. Voigtmann, and M. Laurati, "Binary colloidal glasses: linear viscoelasticity and its link to the microscopic structure and dynamics," Soft Matter **15**, 2232–2244 (2019).